

PSFC/JA-11-34

Production of internal transport barriers via self-generated mean flows in Alcator C-Mod

C. L. Fiore¹, D. R. Ernst¹, Y. A. Podpaly¹, D. Mikkelsen², N. T. Howard¹,
Jungpyo Lee¹, M.L. Reinke¹, J.E. Rice¹, J. W. Hughes¹,
Y. Ma¹, W. L. Rowan³, I. Bespamyatnov³

¹MIT-PSFC, 77 Mass. Ave., Cambridge, MA 02139, USA; fiore@psfc.mit.edu

²Princeton Plasma Physics Laboratory, P.O. Box 451, Princeton, NJ 08543-0451, USA

³FRC, U of Texas at Austin, Austin, TX 78712, USA

December 2011

**Plasma Science and Fusion Center
Massachusetts Institute of Technology
Cambridge MA 02139 USA**

This work was supported by Grant Numbers: US-DoE DE-FC02-99ER54512, DE-FG03-96ER5437 and DE-AC02-09CH11466. Reproduction, translation, publication, use and disposal, in whole or in part, by or for the United States government is permitted.

Production of internal transport barriers via self-generated mean flows in Alcator C-Mod

C. L. Fiore¹, D. R. Ernst¹, Y. A. Podpaly¹, D. Mikkelsen², N. T. Howard¹,
Jungpyo Lee¹, M.L. Reinke¹, J.E. Rice¹, J. W. Hughes¹, Y. Ma¹, W. L. Rowan³,
I. Bespamyatnov³

¹MIT-PSFC, 77 Mass. Ave., Cambridge, MA 02139, USA; fiore@psfc.mit.edu

²Princeton Plasma Physics Laboratory, P.O. Box 451, Princeton, NJ 08543-0451;
mikk@pppl.gov

³FRC, U of Texas at Austin, Austin, TX 78712, USA; w.l.rowan@mail.utexas.edu

New results suggest that changes observed in the intrinsic toroidal rotation influence in the internal transport barrier (ITB) formation in the Alcator C-Mod tokamak [¹E. S. Marmor and Alcator C-Mod group, Fusion Science and Technology **51**, 261 (2007)]. These arise when the resonance for ICRF minority heating is positioned off-axis at or outside of the plasma half-radius. These ITBs form in a reactor relevant regime, without particle or momentum injection, with $T_i \approx T_e$, and with monotonic q profiles ($q_{\min} < 1$). C-Mod H-mode plasmas exhibit strong intrinsic co-current rotation that increases with increasing stored energy without external drive. When the resonance position is moved off-axis, the rotation decreases in the center of the plasma resulting in a radial toroidal rotation profile with a central well which deepens and moves farther off-axis when the ICRF resonance location reaches the plasma half-radius. This profile results in strong $E \times B$ shear ($> 1.5 \times 10^5$ Rad/sec) in the region where the ITB foot is observed. Gyrokinetic analyses indicate that this spontaneous shearing rate is comparable to the linear ion temperature gradient (ITG) growth rate at the ITB location and is sufficient to reduce the turbulent particle and energy transport. New and detailed measurement of the ion temperature demonstrates that the radial profile flattens as the ICRF resonance position moves off axis, decreasing the drive for ITG the instability as well. These results are the first evidence that intrinsic rotation can affect confinement in ITB plasmas.

I. INTRODUCTION

Internal transport barriers (ITB) have been found in many toroidal plasma devices^{2,3} and provide regions of reduced energy, particle, and/or momentum transport in the plasma core. The enhancement of core plasma pressure typically seen in ITB plasmas is attractive as a means of optimizing the fusion power output of magnetic confinement based fusion reactors, but it is not clear if the necessary conditions to produce them can be achieved at reactor conditions. Most commonly, transport barriers in the plasma interior are found in neutral beam heated plasmas^{4,5,6,7,8} where the beam provides a source of particles, momentum and energy to the plasma, which will not be feasible in reactor scale experiment due to the high densities required. The neutral beam induces rotation in the plasma that generates sufficient electromagnetic shear to stabilize the ion temperature gradient driven instability (ITG) as has been observed in numerous experiments^{9,10,11,13}. In cases where ITBs are seen with balanced neutral beam injection (minimal external torque) early beam heat freezes reversed or weak magnetic shear and provides strong core fueling^{3,7,8,10}.

The Alcator C-Mod experiment provides a reactor relevant conditions in which to study ITB physics in several aspects. The sole source of heating to the plasma other than from the ohmic current is provided by up to 8 MW of balanced ICRF power. Thus there is neither momentum input nor particle input into the plasma. The observed rotation arises spontaneously and is entirely intrinsic in origin¹⁴. The C-Mod target plasmas used for these studies are very high density, typically $2 \times 10^{20}/\text{m}^3$ before the ITB is induced, and the ions and electrons are thermally equilibrated. The q-profile is monotonic with q_{min} less than one at the center, as evidenced by sawtooth activity before and during ITB development¹⁵.

Internal transport barriers induced by off-axis ICRF heating in Alcator C-Mod were first reported by in 2001¹⁶, and it was noted then that a significant slowing of the intrinsic central rotation occurred in concert with the ITB development. Gyrokinetic simulation of C-

Mod plasmas demonstrated that the ITG mode fluctuations dominate the particle diffusion in the target plasmas used for ITB study¹⁷. The ion temperature and rotation measurements available prior to 2007 lacked sufficient temporal and spatial resolution to resolve whether the change in the toroidal angular momentum was a cause or a result of the ITB formation. Subsequent experimental and gyrokinetic examination of the onset conditions for ITB development in Alcator C-Mod sought to answer this question. Initial gyrokinetic simulations concluded that the ion temperature profile that occurs with off-axis heating is broad enough to reduce the ITG drive term that dominates the transport in these high density plasmas^{18,19}. The Ware pinch was shown sufficient to account for the slow density peaking that occurs over tens of energy confinement times¹⁹. The work of Zhurovich *et al.*²⁰ supported this conclusion and demonstrated how the change in ICRF resonance position affects the ion temperature profiles and resulting turbulence driven flux. Zhurovich was also able to demonstrate with gyrokinetic modeling that the small magnetic shear found in the core region of Alcator C-Mod was not significant in suppressing the ITG instability in these plasmas. Neither of these studies incorporated rotational shear in the analysis because detailed experimental profiles were not available. Another weakness was that the ion temperature profiles used in both of these studies were not directly measured but were calculated with the power balance code TRANSP²¹, using the ICRF power deposition profiles from TORIC²² and matching the measured neutron rate.

Recently, installation of a high resolution imaging x-ray spectrometer system²³ has allowed accurate and detailed measurement of core toroidal rotation and ion temperature profiles. The results of these measurements obtained for ITB plasmas enhance the ability to perform meaningful gyro-kinetic simulation and to provide an understanding of the relative roles of ion temperature gradient drive and $E \times B$ shearing suppression of turbulence in these plasmas.

In this paper we present details of the new experimental results with a focus on the generation of radial electric field and increased $E \times B$ shear in the ITB formation. These results are used in both linear and non-linear gyrokinetic simulations to investigate the plasma micro-stability of the turbulent driven plasma transport. Gyrokinetic results are compared with experimentally derived transport coefficients.

II. ALCATOR C-MOD ITBs

The ITBs that are observed in C-Mod plasmas ($R=0.69$ m, $a=0.21$ m) have highly peaked pressure and density profiles. They arise after an enhanced D_α H-mode (EDA) has been formed in cases where the net central power is not peaked on axis, as occurs with off-axis ICRF heating and often ohmic H-mode plasmas. Once established, the ITB typically lasts for as much as 10 energy confinement times, until the H-mode plasma undergoes a back transition to L-mode. Variation of the magnetic field is used to move the resonance position of the ICRF heating power, which is available at a fixed frequency. For the experiments described in this paper the ICRF frequency was set to either 70 or 80 Mhz and the toroidal field was used to scan the resonance across the width of the plasma from $r/a=0.57$ (low field side) to $r/a=-0.58$ (high field side.) The plasma current was varied with the magnetic field in order to maintain constant q_{95} . It has been established²⁴ that the ITB foot position moves inversely with changing q_{95} , so it is important to hold this value constant when comparing stability of different discharges. While the ITB foot is found near the ICRF resonance, its location does not correlate well with the position of the ICRF power deposition and rather corresponds most closely to the location of $q=4/3$.

A. Density, Temperature and Pressure Profiles

Fig. 1.a shows an example of the density profile from one of the ITBs used in this study measured with Thomson scattering, which is then fitted with a cubic b-spline routine in the core and a tanh function in the pedestal. The peaking of the density indicates that a

strong barrier to particle transport has formed. The pressure profile also displays strong gradients as is seen in Fig. 1.b. This implies that no loss in thermal energy is occurring as the core density rises and indicates that a thermal barrier exists in the plasma interior as well.

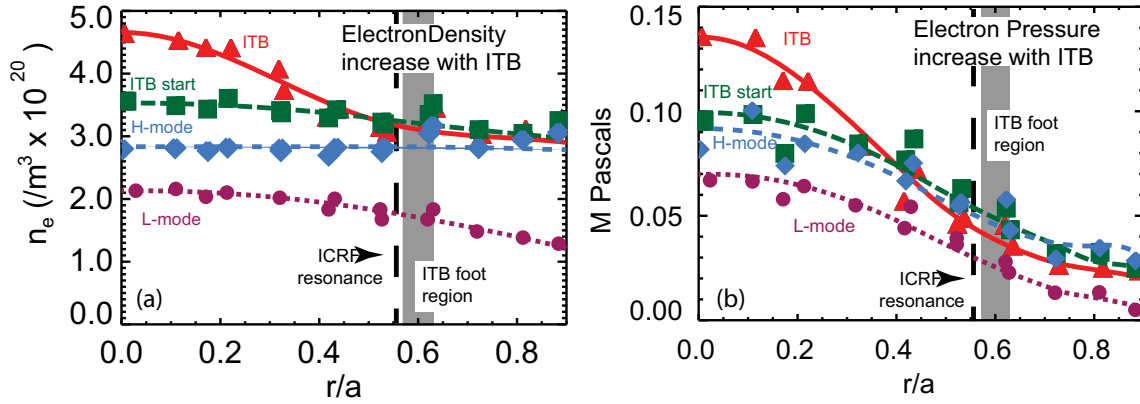


Fig 1 a.) (Color on-line) Density profile in C-Mod ITB plasma with off-axis ICRF heating as the profile transitions from L-mode (purple •) to H-mode (blue ♦) then as the ITB develops (green ■) to becomes established (red ▲). The dashed line represents the location of the ICRF resonance and the region where the ITB foot occurs is shaded. b.) The electron pressure profile from Thomson scattering is shown at the same times as those Fig 1.a.

Ion and electron temperatures, shown in Fig. 2, do not typically increase in the center with the ITB. The fact that they do not decrease as the density rises indicates that the barrier that develops limits thermal transport as well as particle transport. The ion temperature profiles are derived from the broadening of argon and molybdenum lines recorded by an array of von Hamos type x-ray crystal spectrometers²⁵ and an imaging Johann x-ray spectrometer system (HIREX)²³. The electron temperature profiles are from Thomson scattering, and the central T_i is obtained by inverting the global neutron rate using the Thomson electron density profiles and average Z_{eff} .

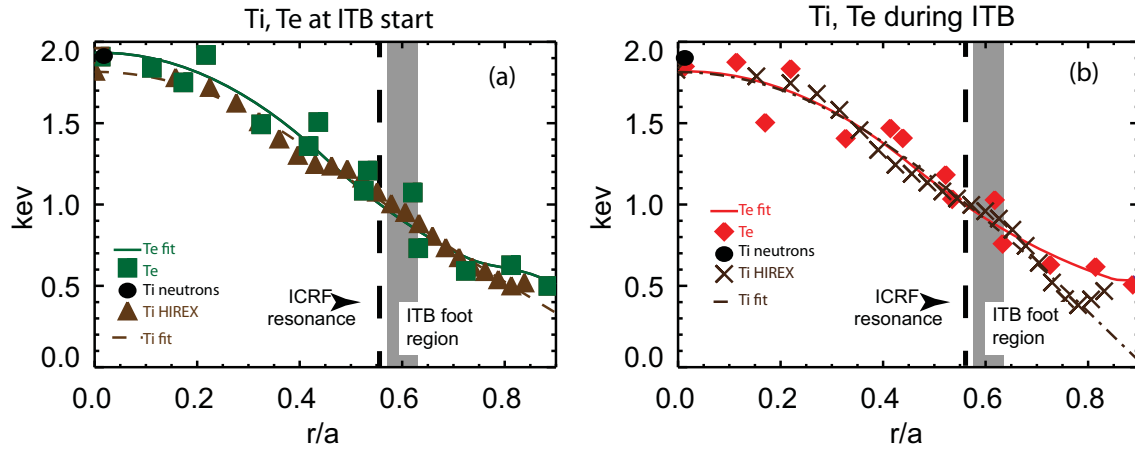


Fig. 2. (Color on-line) Ion and electron temperature profiles a.) at the start of an ITB and b.) after the ITB is established. T_i from x-ray emission is given by black triangles (left), black X (right), dashed line fit to data. T_e is shown as green squares (left), red triangles (right), solid line fit to data. The solid black dot at the center of each plot is central T_i from neutrons. The ITB foot location is marked by the band, and the ICRF resonance by the vertical black line.

Details of prior experimental and modeling analyses of Alcator C-Mod ITBs are summarized in a recent review paper²⁶.

B. Rotation and radial electric field profiles

Toroidal and poloidal rotation data in the core ($r/a < 0.7$) of Alcator C-Mod are obtained from the Doppler shifted x-ray impurity lines of argon and molybdenum, most commonly $^{40}\text{Ar}^{16}$ using the spectrometers mentioned in the previous section. Rotation data from active charge exchange recombination spectroscopy (CXRS) are in good agreement with the x-ray data when available. The spontaneous plasma rotation in Alcator C-Mod is typically in the counter current direction in L-mode, but becomes strongly co-going and centrally peaked after the transition to H-mode. With a typical EDA H-mode plasma created with the ICRF resonance on-axis, this rotation remains centrally peaked and proportional to the plasma stored energy throughout the H-mode. Placing the ICRF resonance off-axis tends to cause the

toroidal rotation to peak off-axis. If the resonance is at $r/a=0.5$ or larger, an ITB usually develops in the plasma, and the central rotation declines, forming a well in the core of the plasma. This change in the velocity trend appears before the peaking in the density that arises with an ITB is evident. A typical rotation profile from an ITB plasma can be seen in Fig. 3. The presence of the rotational well suggests that significant $E \times B$ shear could be developing with the ITB formation. Error on the rotation is typically shown as that from the diagnostic counting statistics which typically range from 1% in the core to 15% in the region of $r/a=0.8$. There is also an absolute level uncertainty which is corrected either by comparison with a discharge containing a locked mode taken the same day, or by comparison with the frequency of $m=1$ sawtooth precursor oscillations. The latter method was employed on the data used in this paper. The offset uncertainty does not significantly affect the shearing rate calculation used for the simulations. The increasing uncertainty with radius can result in 25 to 50% spread in the values of the shearing rate obtained at the ITB foot position over the range of time where the ITB is becoming established.

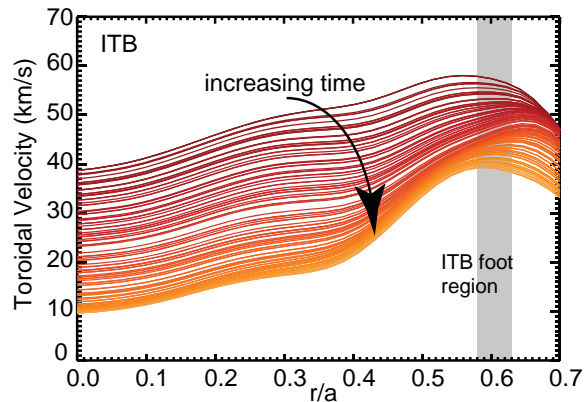


Fig. 3 (Color) The toroidal rotation as a function of radius is shown for an off-axis heated plasma as an ITB develops, beginning at the H-mode transition (dark red) and proceeding until the ITB is established (bright orange).

The experimental parameters are used in the power balance code TRANSP²⁰ in conjunction with the general geometry neoclassical code NCLASS²⁷ to determine the rotation profiles of all remaining plasma species and to derive the radial electric field. The resulting $E \times B$ shearing rate is then calculated.

The total radial electric field for a centrally heated H-mode plasma (no ITB) as a function of radius is displayed in Fig. 4.a including the contributions from the toroidal rotation, the neoclassical poloidal rotation, and the plasma pressure. The largest of these is the toroidal rotation component. (These results were initially discussed in^{28,29}.) The poloidal rotation was less than the measurement threshold for the HIREX diagnostic, consistent with the neoclassical calculation. The E_r reaches a maximum value of 50 kV/m at $r/a \sim 0.45$. In contrast, in an off-axis ICRF heated discharge in which an ITB has developed, the radial electric field is near zero at the center and rises to a value of 20 kV/m in (Fig. 4.b) off center at and outside of the foot of the ITB. Again the component from the toroidal rotation makes up the dominant contribution to the radial electric field despite the increased peaking of the plasma pressure.

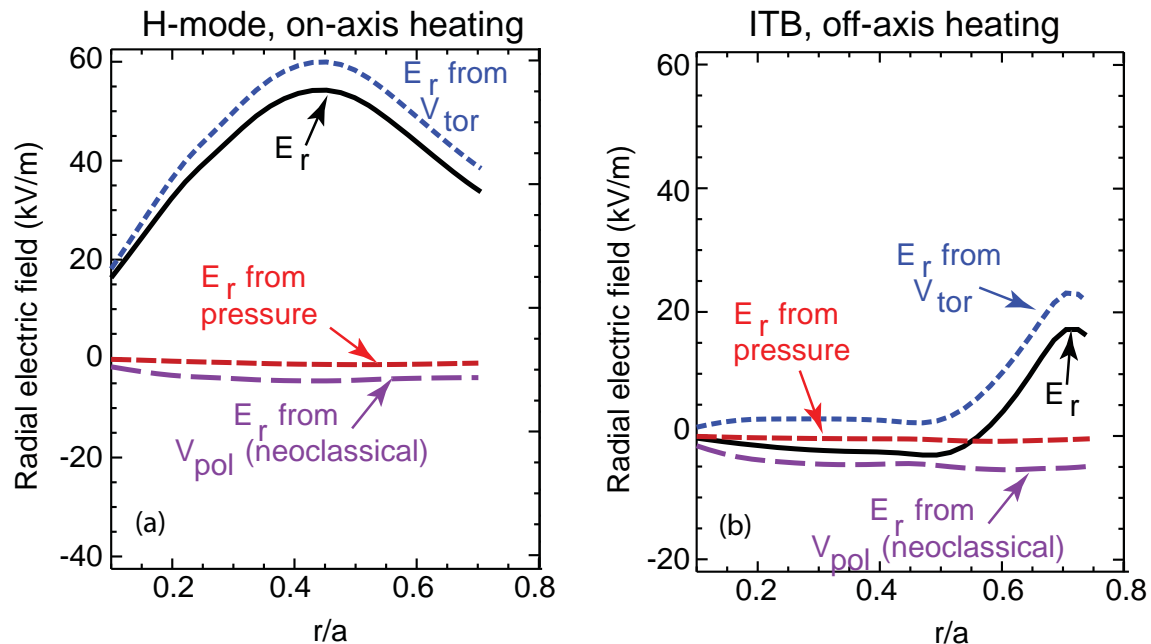


Fig. 4. (Color on-line) The components of the radial electric field derived from the impurity rotation for a.) centrally ICRF heated EDA H-mode plasma and b.) off-axis ICRF heated EDA H-mode plasma with an ITB; total radial electric field (black), pressure term (red), poloidal velocity term (purple), toroidal rotation term (blue).

The resulting $E \times B$ shearing rate (Hahm-Burrell formulation³⁰), displayed in Fig 5, demonstrates that the shearing rate is significantly higher in the region where the ITB foot is observed than at any radial point in the on-axis heated case. The $E \times B$ shearing rate in off-axis heated H-mode plasmas that fail to develop an ITB is also lower than in ITB cases, as can be seen in Fig. 5.b.

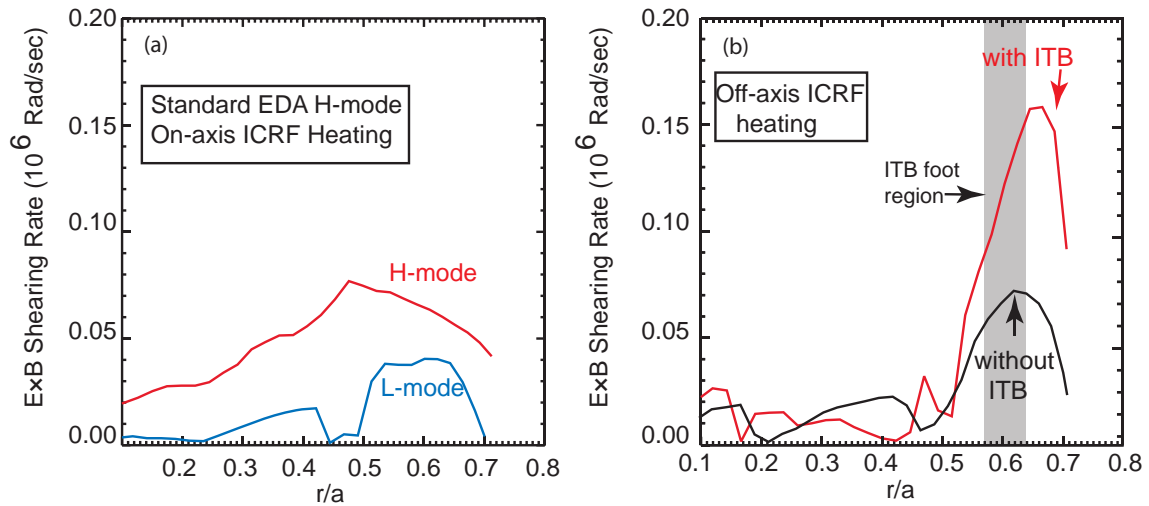


Fig. 5 (Color on-line) The $E \times B$ shearing rates for a) on-axis heated H-mode (red) and L-mode (blue) are compared with that from b) off-axis heated H-mode with ITB (red). An off-axis heated discharge that did not form an ITB (black) is included in b).

C. The effect of temperature gradient on ITB development

ITB development in Alcator C-Mod is coincident with reduction in the outward thermal and particle transport of ions and electrons in the region of the barrier foot. The peaking of the density in the plasma center, inside of the barrier region is consistent with the magnitude of the neoclassical Ware pinch calculated for the experimental plasma parameters. The dominant source of thermal diffusion in high density C-Mod plasmas in the ITB formation phase is expected to be micro-turbulent fluctuations driven by temperature gradients, especially the ion temperature gradient instability (ITG)¹⁹.

Initial gyrokinetic simulations of the off-axis ICRF C-Mod plasmas that developed ITBs have indicated that a reduction of ion temperature gradient reduces the drive for the ITG and leads to a larger stable region in the plasma core²⁰. At the time these simulations were done, measurements of the full radial profiles of the ion temperature were not available, and the simulations were done either by substituting the electron temperature profiles for the ion temperature profiles or by using TRANSP generated ion temperature profiles that used feedback on the χ_i multiplier and the input power profiles to match the measured neutron rate. Both methods indicated that the temperature gradients were reduced as the ICRF resonance is moved off-axis.

In a recent experiment designed to explore the effect of the ICRF resonance position on the ion temperature and plasma rotation profiles, and ultimately the effect on the stability of the plasma, the ICRF resonance was moved across the plasma by scanning the toroidal magnetic field. The ICRF frequency used was fixed at 70 Mhz, so that changing the magnetic field on a shot by shot basis from 5.5 T to 3.9 T moved the ICRF resonance position from $r/a=0.57$ (low field side) to $r/a=-0.58$ (high field side). The plasma current was decreased with the magnetic field to maintain constant q_{95} . Standard EDA H-mode plasmas developed in all cases, but those with the ICRF resonance at $|r/a| \geq 0.5$ developed an ITB after the H-mode transition.

The ion and electron temperature gradients are reduced in the plasma core when the ICRF resonance is off-axis at $|r/a| \geq 0.4$. R/L_{Ti} (Fig 6.a) and R/L_{Te} (Fig 6.b) in an off-axis heated discharge with an ITB to those of a standard centrally heated H-mode are compared. R is the position in major radius while L_{Tx} is the temperature gradient scale length $\left| \frac{1}{T_x} \frac{\partial T_x}{\partial r} \right|^{-1}$.

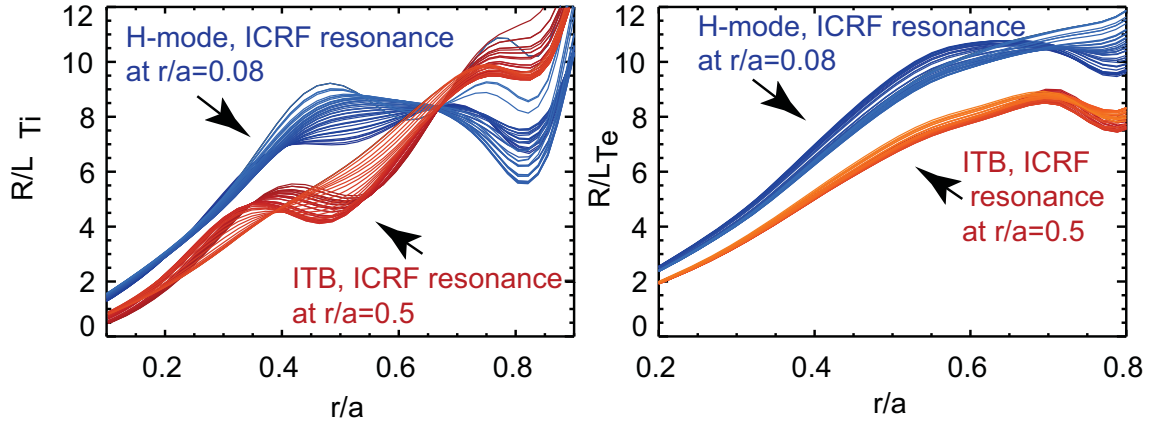


Fig 6. (Color on-line) The dimensionless ion temperature gradient R/L_{Ti} (a) for on-axis heated H-mode plasma (blue) is compared with the off-axis heated H-mode plasma with ITB (red). R/L_{Te} values for the same plasma are compared in (b). Data are shown for multiple time points spanning 0.1 s in the discharge.

To examine the effect of the resonance position on the temperature gradients for the full toroidal field scan, the data are averaged over the temporal extent of the H-mode or ITB. The value of R/L_{Ti} at two radial locations as a function of absolute value ICRF resonance position are shown in Fig. 7. There appeared to be no difference in whether the data arose from an ICRF resonance position on the high field side of the plasma or the low field side, so the absolute value of the resonance position is shown here. While the value of R/L_{Ti} is clearly reduced when the resonance is greater than $|r/a| \geq 0.4$ at inner radii ($r/a=0.25$ is shown in 7.a), it is not obvious at higher radii ($r/a \geq 0.4$ in 7.b). The ITB foot region in this case was at $r/a \approx 0.6$. Error bars in this figure represent the highest and lowest value of R/L_{Ti} in the time range that is used to calculate the average value, which is the data point. Thus the error bars are not symmetric.

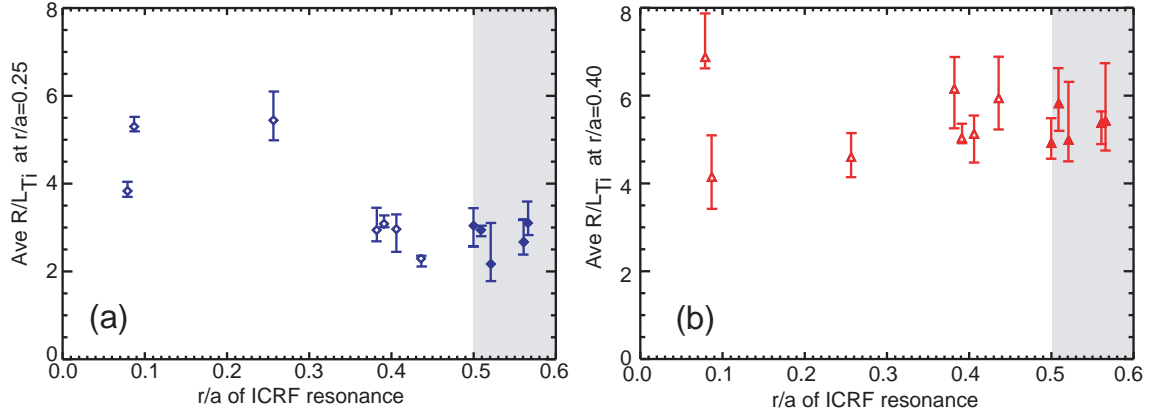


Fig. 7. (Color on-line) R/L_{Ti} as a function of the absolute value of the ICRF resonance position is shown for a) the plasma core at $r/a=0.25$ (blue diamonds) and b) at $r/a=0.40$ (red triangles). The solid symbols indicate that the plasma had an ITB. The shaded area represents the ICRF resonance positions where ITBs are expected to form in H-mode plasmas.

III. RESULTS OF GYROKINETIC ANALYSES

Several gyrokinetic codes have been used to assess the stability of the measured plasma parameters in the off-axis ICRF heated discharges with ITB and also on-axis standard H-mode plasmas. The goal is to examine the role of the ion temperature gradient drive for ITG instability in Alcator C-mod ITBs and also how the stabilizing effects of the spontaneous rotation affects the ITB development in these plasmas.

The initial value gyrokinetic code GS2³¹ has been used in linear simulations to determine the maximum linear growth rate of the ion temperature gradient driven modes in the range of $0 < k_{\theta} \rho_s < 1$ for the off-axis heated H-mode plasmas with ITB included in this paper. An example shown in Fig. 8 demonstrates that the simulated growth rates are comparable to the $E \times B$ shearing rate determined from the measured rotation in the ITB case. The foot of the ITB in this case is found at $r/a \sim 0.6$, which in this case is the radial position where the maximum linear growth rate and the $E \times B$ shearing rate are equal. After the ITB

becomes established, the $E \times B$ shearing rate exceeds the maximum linear growth rate in the outer part of the plasma.

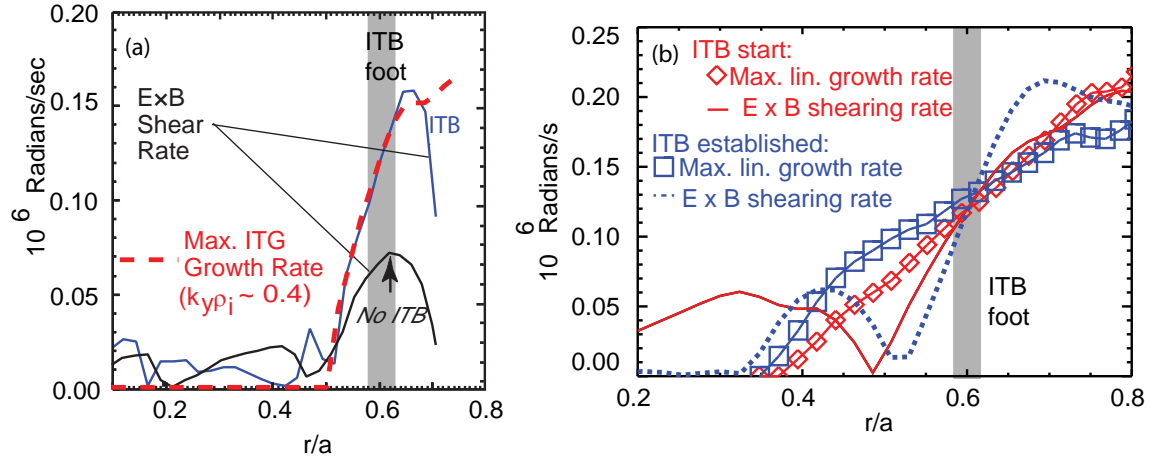


Fig. 8. (Color on-line) The maximum linear growth rate from linear GS2 simulation compared to the experimental $E \times B$ shearing rate in an off-axis heated ITB for a) for a case where T_i was calculated in TRANSP and for b) a case where measured T_i profiles are used in the simulation. Symbols at the time that the ITB starts (red diamonds), when the ITB is fully established (blue squares) and the solid lines that represent the $E \times B$ shearing rates at the same times. Fig 8.a includes an off-axis heated discharge with no ITB (black).

Similarly, the maximum linear growth rate was calculated using the continuum gyrokinetic code GYRO^{32,33} to compare the ITG stability in an on-axis heated H-mode discharge to that of the off-axis heated H-mode with ITB. The maximum linear growth rate is found to be significantly higher in the plasma core for the centrally heated case, and is well above the $E \times B$ shearing rate found for that plasma. Fig.9 shows the results for the on- and off-axis heated plasmas. The results for the off-axis ITB case agree with GS2 calculations for the same plasma discharge.

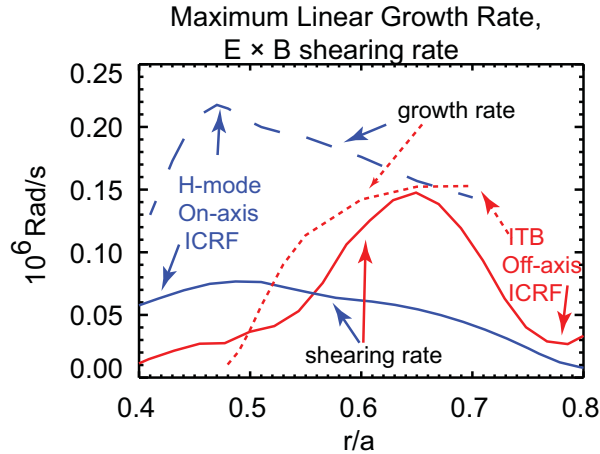


Fig. 9. (Color on-line) The maximum linear growth rate for an on-axis heated H-mode plasma (dashed blue line) is compared to that of an off-axis heated ITB (dashed red). The solid lines are the E×B shearing rates found in the same discharges.

Non-linear (local) simulation using GYRO for the off-axis heated discharge in Fig. 10 was initially carried out with the plasma rotation input disabled. The parameters used for input were the nominal values from the TRANSP processed experimental data without adjustment. The conditions at the time of the simulation are at $t=1.0$ s, which is when the ITB is visibly established in the data, but before strong peaking of the density profile has occurred, and $R/L_n = 2$ at the ITB location, so that the ITG is the dominant instability. Once the fluctuation level calculation converged, the plasma rotation was enabled with the experimentally measured value. A substantial decrease in the simulated χ_i was seen in the simulation after the addition of the addition of rotation, as can be seen in Fig. 10. The mean value of χ_i decreased from $1.2 \text{ m}^2/\text{s}$ to $0.57 \text{ m}^2/\text{s}$, more than a factor of 2 when the rotation was turned on after 800 time steps.

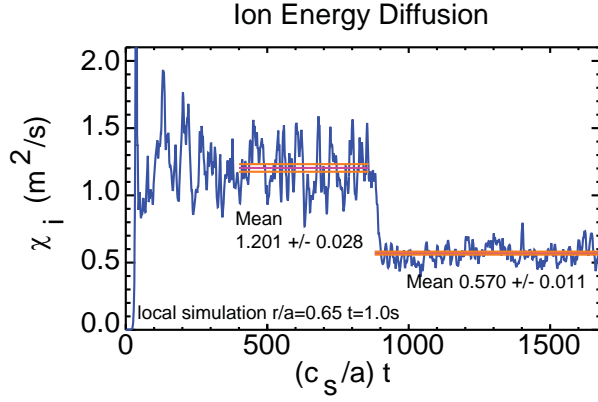


Fig 10. (Color on-line) χ_i from non-linear (local) GYRO simulation with no rotation applied before $t=800$, and with the experimental intrinsic rotation applied at after $t=800$.

The simulated χ_i can be compared with the experimental χ_i values determined with the TRANSP code. The simulated value without rotation included is above the experimental value of $\chi_i = 0.4 \text{ m}^2/\text{s}$ and $\chi_{\text{eff}} = 0.8 \text{ m}^2/\text{s}$ at $t=1.0 \text{ s}$ (because of uncertainty in the ion-electron exchange term when $T_i \approx T_e$, χ_{eff} should be considered as the thermal diffusivity, where

$$\chi_{\text{eff}} \equiv \frac{n_e \chi_e \nabla T_e + n_i \chi_i \nabla T_i}{n_e \nabla T_e + n_i \nabla T_i}. \quad \text{The inclusion of the spontaneous rotation reduces the}$$

simulated χ_i to $0.57 \text{ m}^2/\text{s}$ which lies between the experimental χ_i and χ_{eff} (Fig. 11).

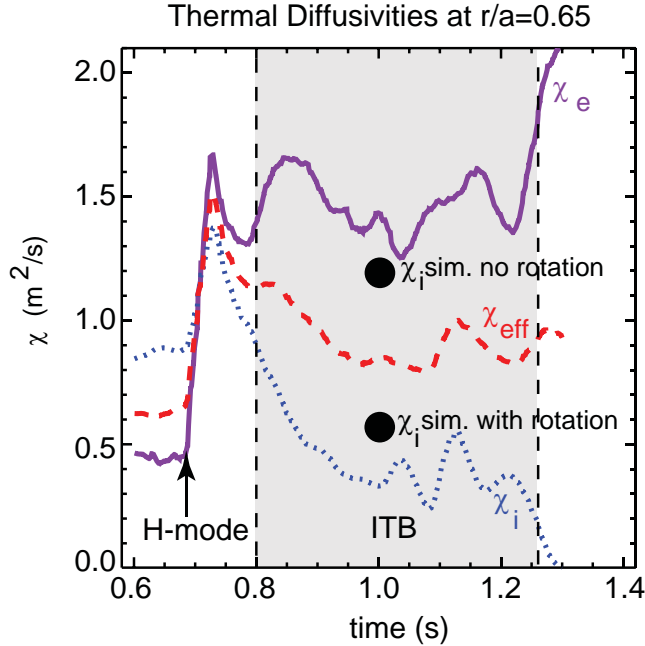


Fig. 11. (Color on-line) TRANSP calculation of the thermal diffusivities for the off-axis heated H-mode with ITB that is used in the GYRO simulation of Fig 10 are χ_i (dotted blue), χ_{eff} (dashed red) and χ_e (solid purple). Simulated χ_i values (black dots) with and without rotation are included.

From the time when the H-mode forms shown in Fig. 11 to $t=1.0\text{s}$ when the simulations have been done and the ITB has formed, the value of χ_i at $r/a=0.65$ decreases by a factor of 4.

Examination of the value of χ_i determined for variations of several plasma parameters within the expected error of 10% finds that χ_i lies between 0.2 and 0.5 m^2/s . The value of the neoclassical χ_i for several different formulations lies between 0.1 and 0.4 m^2/s . The χ_i thus achieved during the ITB is essentially at the neoclassical level.

IV DISCUSSION

The formation of ITBs in many toroidal experiments is attributed to stabilization of ITG turbulence through induced $E \times B$ shear resulting from the application of directed neutral beams and the inherent toroidal rotation that arises. Because there are no neutral beams or other external sources of momentum input to C-Mod, an explanation of the ITB formation

initially focused on the reduction the thermal gradients that drive the ITG, and it was concluded that this increased stability could account for the reduction of thermal diffusion that occurs in these plasmas. Direct measurement of the ion temperature radial profiles through improved capability in the diagnostics indicates that the gradients are reduced in the off-axis heated plasmas that produce ITBs. The linear growth rate calculations show that the instability growth is lower in ITB plasmas. However, the non-linear simulation using the experimentally derived parameters suggests that this reduction is not sufficient to reproduce the experimental diffusivity values observed in the ITB.

New measurement of the spontaneous plasma rotation profile indicates that it produces $E \times B$ shearing rates comparable to the maximum linear growth rate in the ITB foot region, and thus should be considered as a possible mechanism for stabilization of the ITG in the ITB plasmas. Indeed the non-linear gyrokinetic simulation that includes this spontaneous rotation does allow reproduction of the experimental thermal diffusivity values.

It is likely that the appearance of the reduced diffusivity that is the hallmark of the ITB in C-Mod plasmas requires both the reduction of the ITG linear growth rate that results from the reduced ion temperature gradient and also the presence of the spontaneous $E \times B$ shearing rate arising from the intrinsic rotation.

V. Summary and Future Work

Alcator C-Mod is unique in displaying the presence of internal transport barrier development in H-mode plasmas with monotonic q -profiles ($q_{\min} \leq 1$) without the introduction of external torque or core fueling to the plasma. A strong co-current intrinsic rotation develops in all C-Mod plasmas following the H-mode transition, but decreases in the plasma center when the ICRF resonance and resulting heating is off-axis. The decrease in the center does not affect the rotation outside of the half radius so that a well in the rotation profile appears, which leads

to increased $E \times B$ shear in the region where ultimately an ITB forms. The observed shearing rate is 2 to 3 times higher than what is seen in on-axis heated H-mode discharges that do not form an ITB.

While a reduction in the maximum linear growth rate is seen in ITB plasmas due to flattening of the ion temperature profile and reduction of the ion temperature gradient, non-linear gyrokinetic simulation suggests that it is not sufficient to produce the experimental thermal diffusivities, and that the additional stabilization provided by the spontaneous rotation profile is necessary.

Exploring these phenomena with further gyrokinetic simulations will be the focus of continued study in this area. Examination of parametric dependencies of the stability within experimental errors are required to have complete confidence in the conclusions reached here, which requires a large investment in computational time.

Given the projections that have been made for intrinsic rotation in ITER, extrapolation of these results to ITER will be of great interest to the community.

ACKNOWLEDGEMENTS

The authors are indebted to John Wright, Ted Baker, and Paul Bonoli for providing use of the LOKI computer cluster for use in the simulations, and also to Anne White and Martin Greenwald for useful discussions. Access to the GYRO code was provided by Jeff Candy and Ron Waltz of General Atomics. The authors would also like to acknowledge the assistance and support of the C-Mod experimental staff. This work was supported by US-DoE DE-FC02-99ER54512, DE-FG03-96ER5437 and DE-AC02-09CH11466.

REFERENCES

- ¹E. S. Marmor and Alcator C-Mod group, Fusion Science and Technology **51**, 261 (2007)
- ²R. C. Wolf, Plasma Phys, and Control. Fusion **45**, R1 (2003).

- ³J.W. Connor, T. Fukuda, X. Garbet, C. Gormezano, V. Mukhovatov, M. Wakatani, the ITB Database Group, the ITPA Topical Group on Transport and Internal Barrier Physics, Nucl. Fusion **44** R1 (2004).
- ⁴F. M. Levinton, M. C. Zarnstorff, S. H. Batha, M. Bell, R. E. Bell, R. V. Budny, C. Bush, Z. Chang, E. Fredrickson, A. Janos, J. Manickam, A. Ramsey, S. A. Sabbagh, G. L. Schmidt, E. J. Synakowski, and G. Taylor, Phys. Rev. Lett. **75**, 4417 (1995).
- ⁵E. J. Strait, L. L. Lao, M. E. Mauel, B. W. Rice, T. S. Taylor, K. H. Burrell, M. S. Chu, E. A. Lazarus, T. H. Osborne, S. J. Thompson, A. D. Turnbull, Phys. Rev. Lett. **75**, 4421 (1995).
- ⁶T. Fujita, S. Ide, H. Shirai, M. Kikuchi, O. Naito, Y. Koide, S. Takeji, H. Kubo, and S. Ishida, Phys. Rev. Lett. **78**, 2377 (1997).
- ⁷O. Gruber, R. C. Wolf, R. Dux, C. Fuchs, S. Günter, A. Kallenbach, K. Lackner, M. Maraschek, P. J. McCarthy, H. Meister, G. Pereverzev, F. Ryter, J. Schweinzer, U. Seidel, S. Sesnic, A. Stäbler, J. Stober, and the ASDEX Upgrade Team, Phys. Rev. Lett. **83**, 1787 (1999).
- ⁸Y. Koide, M. Kikuchi, M. Mori, S. Tsuji, S. Ishida, N. Asakura, Y. Kamada, T. Nishitani, Y. Kawano, T. Hatae, T. Fujita, T. Fukuda, A. Sakasai, T. Kondoh, R. Yoshino, and Y. Neyatani, Phys. Rev. Lett. **72**, 3662 (1994).
- ⁹E. J. Synakowski, S. H. Batha, M. A. Beer, M. G. Bell, R. E. Bell, R. V. Budny, C. E. Bush, P. C. Efthimion, G. W. Hammett, T. S. Hahm, B. LeBlanc, F. Levinton, E. Mazzucato, H. Park, A. T. Ramsey, G. Rewoldt, S. D. Scott, G. Schmidt, W. M. Tang, G. Taylor, and M. C. Zarnstorff, Phys. Rev. Lett. **78**, 2972 (1997).
- ¹⁰K. H. Burrell, Phys Plasmas **4**, 1499 (1997).
- ¹¹Y. Sakamoto, Y. Kamada, S. Ide, T. Fujita, H. Shirai, T. Takizuka, Y. Koide, T. Fukuda, T. Oikawa, T. Suzuki, K. Shinohara, R. Yoshino and JT-60 Team, Nucl. Fusion **41**, 865 (2001).
- ¹²P.C. de Vries, E. Joffrin, M. Brix, C.D. Challis, K. Crombé, B. Esposito, N.C. Hawkes, C. Giroud, J. Hobirk, J. Lönnroth, P. Mantica, D. Srintzi, T. Tala, I. Voitsekhovitch and JET-EFDA Contributors to the Work Programme, Nucl. Fusion **49**, 075007 (2009).
- ¹³M. W. Shafer, G. R. McKee, M. E. Austin, K. H. Burrell, R. J. Fonck, and D. J. Schlossberg, Phys. Rev. Lett. **103**, 075004 (2009).
- ¹⁴J.E. Rice, P.T. Bonoli, J.A. Goetz, M.J. Greenwald, I.H. Hutchinson, E.S. Marmor, M. Porkolab, S.M. Wolfe, S.J. Wukitch and C.S. Chang, Nucl. Fusion **39**, 1175 (1999).
- ¹⁵C. L. Fiore, J. E. Rice, P. T. Bonoli, R. L. Boivin, J. A. Goetz, A. E. Hubbard, I. H. Hutchinson, R. S. Granetz, M. J. Greenwald, E. S. Marmor, D. Mossessian, M. Porkolab, G. Taylor, J. Snipes, S. M. Wolfe, S. J. Wukitch, Phys. Plasmas **8**, 2023 (2001).
- ¹⁶J. E. Rice, R. L. Boivin, P. T. Bonoli, J. A. Goetz, R. S. Granetz, M. J. Greenwald, I. H. Hutchinson, E. S. Marmor, G. Schilling, J. A. Snipes, S. M. Wolfe, S. J. Wukitch, C. L. Fiore, J. H. Irby, D. Mossessian, M. Porkolab, Nucl. Fusion **41**, 277(2001).

- ¹⁷ L. Lin, M. Porkolab, E. M. Edlund, J. C. Rost, C. L. Fiore, M. Greenwald, Y. Lin, D. R. Mikkelsen, N. Tsujii, and S. J. Wukitch, *Phys. Plasmas* **16**, 012502 (2009).
- ¹⁸ M. H. Redi, D. R. Mikkelsen, G. Rewoldt, C. Fiore, P. Bonoli, D. Ernst, J. Rice, S. Wukitch, W. Dorland, J. Candy, R. Waltz, *Phys. Plasmas* **12**, 072519-1 (2005).
- ¹⁹ D. R. Ernst, P. T. Bonoli, P. J. Catto, W. Dorland, C. L. Fiore, R. S. Granetz, M. Greenwald, A. E. Hubbard, M. Porkolab, M. H. Redi, J. E. Rice, K. Zhurovich, and Alcator C-Mod Group, *Phys. Plasmas* **11**, 2036 (2004).
- ²⁰ K. Zhurovich, C.L. Fiore, D.R. Ernst, P.T. Bonoli, M.J. Greenwald, A.E. Hubbard, J.W. Hughes, E.S. Marmor, D.R. Mikkelsen, P. Phillips and J.E. Rice, *Nucl. Fusion* **47**, 1220 (2007).
- ²¹ R. Hawryluk in *Physics of Plasma Close to Thermonuclear Conditions* (Varenna, 1979), Commission of the European Communities, Brussels, Vol. I p 61 (1979).
- ²² M Brambilla, 1999, *Plasma. Phys. Controlled Fus.* **41**, 1 (1999).
- ²³ A. Ince-Cushman, J. E. Rice, M. Bitter, M. L. Reinke, K. W. Hill, M. F. Gu, E. Eikenberry, Ch. Broennimann, S. Scott, Y. Podpaly, S. G. Lee, E. S. Marmor, *Rev. Sci. Instrum.* **79**, 10E302 (2008).
- ²⁴ C. L. Fiore, P. T. Bonoli, D. R. Ernst, A. E. Hubbard, M. J. Greenwald, A. Lynn, E. S. Marmor, P. Phillips, M. H. Redi, J. E. Rice, S. M. Wolfe, S. J. Wukitch, K. Zhurovich, *Phys. Plasmas* **10**, 2480 (2004).
- ²⁵ J. E. Rice, F. Bombarda, M. A. Graf, E. S. Marmor, and Y. Wang, *Rev. Sci. Instrum.* **66**, 752 (1995).
- ²⁶ C. L. Fiore, D. R. Ernst, J. E. Rice, K. Zhurovich, N. Basse, P. T. Bonoli, M. J. Greenwald, E. S. Marmor, and S. J. Wukitch, *Fusion Science and Technology* **51**, 303 (2007).
- ²⁷ W. A. Houlberg¹, K. C. Shaing², S. P. Hirshman¹, and M. C. Zarnstorf, *Phys. Plasmas* **4**, 3230 (1997).
- ²⁸ J. E. Rice, P. T. Bonoli, C. L. Fiore, W. D. Lee, E. S. Marmor, S. J. Wukitch, R. S. Granetz, A. E. Hubbard, J. W. Hughes, J. H. Irby, Y. Lin, D. Mossessian, S. M. Wolfe, K. Zhurovich, M. J. Greenwald, I. H. Hutchinson, M. Porkolab, J. A. Snipes, *Nucl. Fusion* **43**, 781 (2003).
- ²⁹ C.L. Fiore, J.E. Rice, Y. Podpaly, I.O. Bespamyatnov, W.L. Rowan, J.W. Hughes and M. Reinke, *Nucl. Fusion* **50**, 064008 (2010).
- ³⁰ T. S. Hahm, K. H. Burrell, *Phys. Plasmas* **2**, 1648 (1995).
- ³¹ W. Dorland, F. Jenko, M. Kotschenreuther, and B. N. Rogers, *Phys. Rev. Lett.*, **85**, 5579 (2000).

³² J.Candy and R.E.Waltz, J. Comput. Phys. **186**, 545 (2003).

³³ J. Candy and E.A. Belli, *GYRO Technical Guide*, General Atomics Report **GA-A26818** (2010).